Periodic analysis of urethane-induced pulmonary tumors in living A/J mice by respiration-gated X-ray microcomputed tomography

Yusaku Hori,[1,2] Nobuo Takasuka,[1] Michihiro Mutoh,[1] Tsukasa Kitahashi,[1] Shuji Kojima,[2] Katsumi Imaida,[3] Masahiro Suzuki,[4] Kazushi Kohara,[4] Shuji Yamamoto,[4] Noriyuki Moriyama,[4] Takashi Sugimura[1] and Keiji Wakabayashi[1,5]

[1]Cancer Prevention Basic Research Project, National Cancer Center Research Institute, 5-1-1 Tsukiji, Chuo-ku, Tokyo 104-0045; [2]Department of Radiation Biosciences, Faculty of Pharmaceutical Sciences, Tokyo University of Science, 2641 Yamazaki, Noda-shi, Chiba 278-8510; [3]Onco-Pathology, Department of Pathology and Host-Defense, Faculty of Medicine, Kagawa University, 1750-1 Ikenobe, Miki-cho, Kita-gun, Kagawa 761-0793; [4]Research Center for Cancer Prevention and Screening, National Cancer Center, 5-1-1 Tsukiji, Chuo-ku, Tokyo 104-0045, Japan

(Received March 18, 2008/Revised May 2, 2008/Accepted May 19, 2008/Online publication July 4, 2008)

X-ray microcomputed tomography (micro-CT) with a respiratory gating system is a useful non-invasive approach to evaluate lung tumor development in living animal models. Here micro-CT was applied for the detection of lung lesions induced by a single intraperitoneal injection (250 mg/kg) of urethane in male A/J mice, at 2-week intervals from 10 to 30 weeks after carcinogen exposure. In micro-CT cross sections, lung tumor images were easily distinguished from surrounding non-tumorous tissues, the smallest detected tumor being approximately 0.5 mm in diameter. All of the urethane-treated mice (n = 15) developed lung tumors and the number of tumors developed in each mouse was 8.6 ± 3.9. Six tumors, determined histopathologically to be adenocarcinomas, were detected, growing at different rates during the experimental period. The most aggressive carcinoma, increasing in diameter from 0.9 to 3.5 mm within 8 weeks, was a solid-type nodule with a clear tumor margin on the micro-CT imaging. Other tumors, histopathologically adenomas, grew slowly or moderately. The results provide evidence that micro-CT is a useful non-invasive imaging approach for evaluating the characteristics and growth of lung tumors in mice. (*Cancer Sci* 2008; 99: 1774–1777)

Lung cancer is the leading cause of cancer death worldwide.[1] For detecting lung cancer, X-ray fluoroscopy has been used widely in practical screening. X-ray computed tomography (CT) is also used to detect early stage lesions and to evaluate tumor progression and metastasis during clinical treatment.[2] Moreover, X-ray CT is a useful tool for monitoring lung tumor development in living animal models[3] and major efforts have been invested in developing devices for imaging the inner anatomy of small animals. As with CT for human cases, micro-CT for rodents allows evaluation of bones and other calcified changes as well as diagnosis of soft tissue changes, such as lung tumor development.[4,5] Non-invasiveness, the ability to monitor therapeutic effects, the capacity to optimize the experimental period, and a lowering in the number of animals used can all be considered advantages of this novel approach. However, there are also disadvantages in that it is difficult to make a refined evaluation in very small rodents, and the image quality is strongly affected by motion-related artifacts. Several efforts, particularly the development of a method with a respiratory gating system for obtaining sharper images, have been made to overcome these difficulties.[6–8]

Hitherto, the utility of micro-CT has been reported for detecting lung tumors in a metastatic rodent model, a *K-ras* transgenic lung cancer model, and a urethane-induced mouse lung tumor model.[5,8–10] However, in those reports the mice were scanned only once by micro-CT, and then killed for histopathological analysis of lung lesions. Full utilization of the advantages of respiration-gated micro-CT for periodic detection of sizes in lung tumors and their growth over time has not been made.

In the present study, urethane-induced tumor development was therefore monitored periodically using respiration-gated micro-CT. The results obtained indicate that tumors grow at markedly varying speeds, which may not directly reflect the histopathological findings after autopsy. The necessity for appropriate scanning methods of micro-CT images, which link to histopathology, is discussed in the text.

Materials and Methods

Animals. Male A/J Jms Slc mice (5 weeks old) were purchased from Japan SLC (Hamamatsu, Japan). They were housed five to a plastic cage with woodchip bedding in an airconditioned animal room maintained at 24 ± 2°C and 60 ± 5% relative humidity with a 12:12 h L : D cycle. Basal diet (CE-2; CLEA, Tokyo, Japan) and water were available *ad libitum* throughout the experiment.

Treatment. The experimental protocol is shown in Figure 1. At 6 weeks of age, mice (n = 15) were treated with a single intraperitoneal injection of urethane (250 mg/kg; Sigma, St Louis, MO, USA) in 0.9% NaCl saline. Control mice (n = 10) were given a single saline intraperitoneal injection. The mice were scanned by micro-CT every 2 weeks from 10 to 30 weeks after urethane or control vehicle injection. The experiments were conducted according to the Guidelines for Animal Experiments in National Cancer Center of the Committee for Ethics of Animal Experimentation.

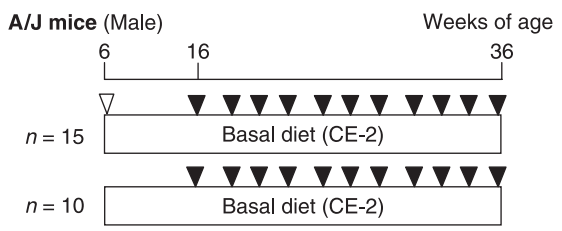

Fig. 1. Experimental protocol. Six-week-old male A/J mice were injected with 250 mg/kg urethane and killed 30 weeks later. During the experimental period, the mice were scanned by microcomputed tomography every 2 weeks from 10 to 30 weeks after urethane injection. ▽, intraperitoneal urethane; ▼, computed tomography scan.

[5]To whom correspondence should be addressed. E-mail: kwakabay@ncc.go.jp

doi: 10.1111/j.1349-7006.2008.00889.x

Table 1. Incidence and multiplicity of lung tumors in A/J mice assessed by microcomputed tomography

Treatment	No. mice	Total tumors detected at 16 weeks		Total tumors detected at 36 weeks	
		Incidence	No. tumors/mouse	Incidence	No. tumors/mouse
Urethane	15	10 (67)	1.6 ± 1.0	15 (100)	8.6 ± 3.9
Vehicle	10	0 (0)	0	0 (0)	0

Data are means ± SD. Numbers in parentheses are the percentages of mice with lung tumors.

Table 2. Incidence and multiplicity of lung tumors in A/J mice assessed histopathologically

Treatment	No. mice	Adenoma		Adenocarcinoma		Total tumors	
		Incidence	No. tumors/mouse	Incidence	No. tumors/mouse	Incidence	No. tumors/mouse
Urethane	15	15 (100)	7.1 ± 3.2	3 (20)	2.0 ± 1.0	15 (100)	9.5 ± 3.8
Vehicle	10	0 (0)	0	0 (0)	0	0 (0)	0

Data are means ± SD. Numbers in parentheses are the percentages of mice with lung tumors.

Micro-CT scan procedure. All mice were anesthetized with isoflurane (Dainippon Sumitomo Pharmaceutical, Osaka, Japan) and maintained anesthesia was achieved with a mixture of isoflurane and room air delivered during the scanning with micro-CT. Each mouse was placed on its back on an animal bed for micro-CT scanning and banded across the chest area, and a sensor for detecting respiration was placed on the abdomen. The X-ray scanning time point was set at 1200 ms after expiration.

For scanning, a new cone-beam micro-CT scanner (eXplore Locus; General Electric Healthcare, London, UK) was used. The scan parameters that are consistent for gated *in vivo* scan acquisitions include: 80 kV peak, 450 μA, 400 ms per frame, 0.5 degrees at the angle of increment, and 720 views. The measured in-air radiation at the isocenter was 240 mGy. Three-dimensional images obtained from axial, sagittal, coronal, and oblique micro-CT images were reconstructed using MicroView (General Electric Healthcare).

Histopathological examination. The mice were killed 30 weeks after urethane administration and the major organs, such as the liver, kidneys, and spleen, were weighed before fixation in 10% buffered formalin. The lungs were inflated for this purpose and lung tumors, detected using a stereoscopic microscope, were embedded in paraffin blocks and sectioned at 3 μm for placement on slides and staining with hematoxylin–eosin for histopathological evaluation. Lung lesions were diagnosed according to the criteria of the *International Classification of Rodent Tumors: Mouse*.[11]

Results

In the micro-CT images, the lung tumors were clearly distinguished from the surrounding non-tumorous tissues. Moreover, reconstructed three-dimensional images easily differentiated the tumors (globular) and blood vessels (tube structure) in the lungs, even though both have a similar X-ray absorption.

The total numbers of lung tumors detected by micro-CT are summarized in Table 1. The smallest detectable tumor was approximately 0.5 mm in diameter and the largest tumor measured 3.5 mm. At 16 weeks, that is 10 weeks after urethane injection, the incidence of tumors detected by micro-CT was 67%, and the number of tumors per mouse detected by micro-CT was 1.6 ± 1.0. The incidence of tumors increased to 100% at the end of the experiment at 36 weeks, with the multiplicity increasing to 8.6 ± 3.9 (Table 1). Table 2 shows the incidence and multiplicity of lung tumors at 36 weeks as determined by histopathological analysis. The incidence of adenoma was 100% and that of adenocarcimoma was 20%, and the numbers of adenomas and adenocarcinomas were 7.1 ± 3.2 and 2.0 ± 1.0 per mouse, respectively.

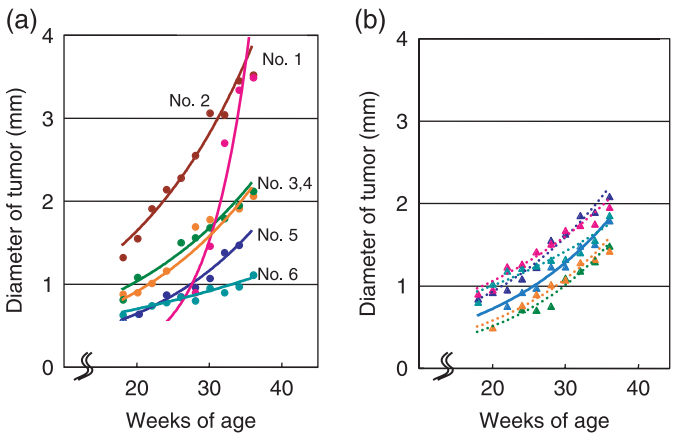

Fig. 2. Increase in pulmonary tumor diameters in A/J mice treated with urethane. (a) Growth curves of six adenocarcinomas (no. 1–6). (b) Growth curves of six representative adenomas. Each tumor scanned by microcomputed tomography was reconstructed to three-dimensional images (axial, sagittal, coronal, and oblique) and maximum diameters were measured periodically.

Figure 2a shows growth curves for all six adenocarcinomas that developed in A/J mice with urethane treatment. One tumor (no. 1) grew particularly rapidly and its diameter increased from 0.9 to 3.5 mm within 8 weeks. This solid-type nodule with a clear tumor margin on CT images is illustrated in Figure 3a–c. The earliest-detected adenocarcinoma (no. 2) grew at a moderate speed from 1.3 to 3.5 mm over 20 weeks, and was solid type with spiked edges on CT (Fig. 3d–f).

Figure 2b shows growth curves for six adenomas that developed in A/J mice with urethane treatment. The diameters of the tumors doubled at the end of the experiment, and the growth speed was almost the same as that of the adenocarcinomas (no. 3–5) shown in Figure 2a. These tumors, which grew moderately, showed clear tumor edges and/or spiked edges in a CT image (Fig. 3g–i). These lung lesions were diagnosed as bronchiolo-alveolar adenomas.

The most rapidly growing tumor (Fig. 2a, no. 1) was histopathologically diagnosed as an adenocarcinoma with poorly differentiated features (Fig. 4a,b), a solid growth pattern without

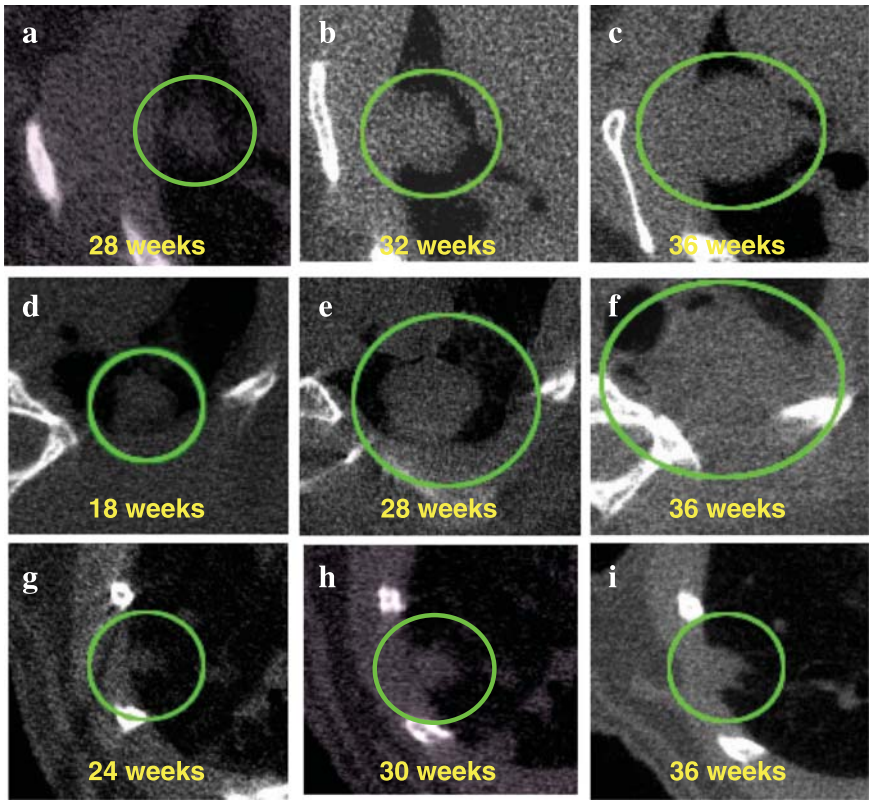

Fig. 3. Virtual *in vivo* microcomputed tomography (micro-CT) images of growing lung tumors. Axial micro-CT images of the thorax of a mouse at the indicated time points are shown. (a–c) The most aggressive lung adenocarcinoma is represented by curve no. 1 in Figure 2a. Micro-CT images, scanned at 28, 32, and 36 weeks of age, are shown. (d–f) The earliest detected lung adenocarcinoma is represented by curve no. 2 in Figure 2a. Micro-CT images, scanned at 18, 28, and 36 weeks of age, are shown. (g–i) One lung adenoma represented by a solid line is shown in Figure 2b. Micro-CT images, scanned at 24, 30, and 36 weeks of age, are shown. Tumors observed in the lung are circled.

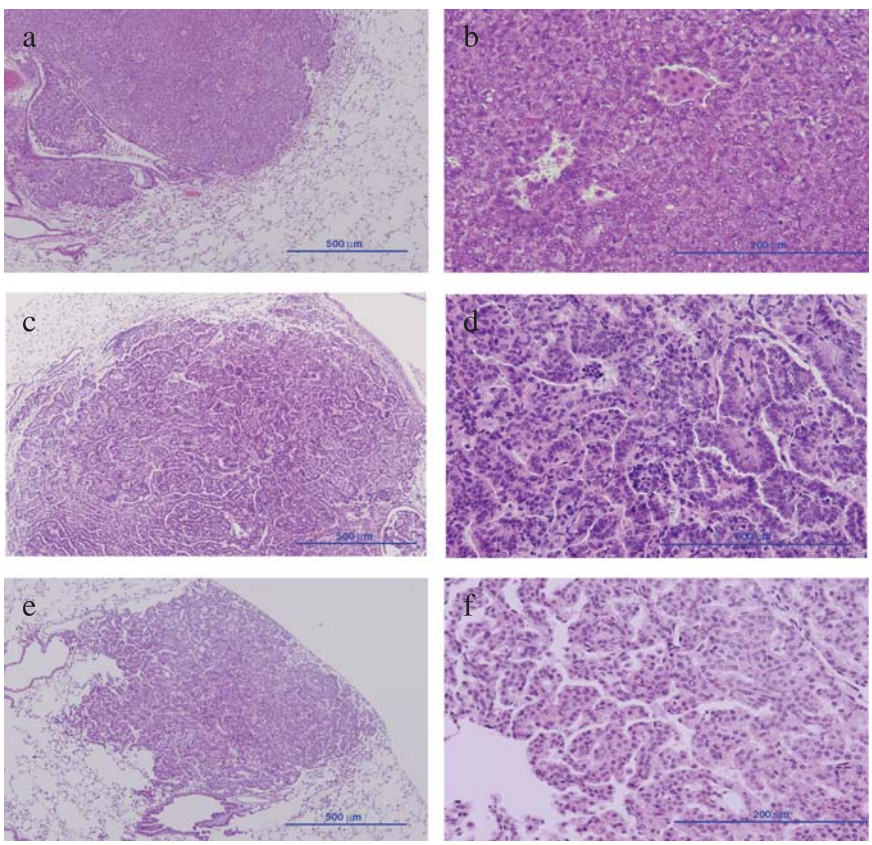

Fig. 4. Histopathological findings for lung tumors developed by urethane treatment. (a,b) The most aggressive lung adenocarcinoma is represented by curve no. 1 in Figure 2a,c,d. The earliest detected lung adenocarcinoma is represented by curve no. 2 in Figure 2a,e,f. One of the lung adenomas represented by a solid line is shown in Figure 2b. (a,c,e) Scale bar = 500 μm; magnification, ×100. (b,d,f) Scale bar = 200 μm; magnification, ×400.

doi: 10.1111/j.1349-7006.2008.00889.x

any glandular or tubular formation, and densely grouped cells with little connective tissue. Nuclei were pleomorphic with condensed chromatin. Mitotic cells were also observed frequently. Histopathology revealed all moderately growing malignancies (no. 2–4) to be adenocarcinomas with papillary formation, even though size differences were obvious between no.2 (Fig. 4c,d) and no. 3–5 (data not shown). The tumor cells had abundant eosinophilic cytoplasm, round to oval-shaped nuclei, and occasional condensed chromatin. The histopathology findings for one slow-growing tumor (no. 6) were 'carcinoma in adenoma'. Figure 4e,f illustrates a papillary-type adenoma. As seen in adenoma, few mitotic cells were observed, its nucleus was oval to round in shape, and condensed chromatin was not observed.

Discussion

In the present study, micro-CT with a respiratory gating system was shown to be useful for evaluating the developmental course of carcinogen-induced lung tumors in mouse models without invasive techniques. We used urethane-induced A/J mouse lung tumor models, because urethane has been applied as a carcinogen for mouse lung tumorigenesis studies for over 60 years and many details have been published.[12] The sensitivity of the A/J mouse is reflected in the occurrence of *K-ras* mutations in lung tumor tissue.[13] Micro-CT images here revealed that the numbers of tumors increased after urethane treatment, but that individual lesions grew differently, with the variation related mainly to histopathological features.

When counting the tumors in lung histopathological sections collected from 36-week-old mice, we found that the total number of tumors in the CT images was slightly lower than that detected by macroscopic study (8.6 per mouse vs 9.5 per mouse). It is likely that lesions in the hilus of the lung or at the periphery might be overlooked and that cardiac motion may also hinder clear imaging.

The smallest tumor detected in the present study was approximately 0.5 mm, consistent with an earlier report.[6] Although the estimated smallest size documented in the literature is 0.2 mm,[5] this was beyond the capacity in living and breathing mice even using a respiratory gating system.

The characterization of early nodules by CT imaging would help to distinguish slow-growing tumors from those growing rapidly. Characteristic micro-CT images may be observed in the shape of tumor edge and inner pattern, but in the present study the image could not show the detail of tumor development. Thus, further improvements in scanning technology are necessary to enable higher-resolution imaging to discern the differences and characteristics of early lesions and lung tumors. Moreover, it is hoped that a clear distinction between adenoma and adenocarcinoma, which grow at similar speeds, can be made by micro-CT imaging. However, at present it is also not possible to discriminate adenomas and carcinomas by micro-CT imaging. It is assumed that technical innovations may overcome these problems in the near future.

In experiments using radiography, the effects of radiation exposure (each exposure was 240 mGy) on tumor development, which could influence the outcome of the experiment, are difficult to eliminate. During our experiment, the control radiation exposure group did not develop lung tumors (Table 1). Moreover, changes in the pulmonary epithelium in response to irradiation, such as cytomegaly, multinucleation, macronucleoli, and cytoplasmic vacuolization, were not observed in either tumorous or non-tumorous lung tissues of mice treated with urethane. Further experiments are needed to clarify the effects of the amount and frequency of radiation exposure on lung tissue. To decrease the level of exposure, we limited the number of views and used half-scan mode, but further improvement in the devices is to be expected.

In conclusion, our results provide evidence that respiratory-gated micro-CT scanning of live mice has potential as a method for evaluating the growth of lung tumors. Micro-CT has the advantage of being highly sensitive compared to ultrasonography and magnetic resonance imaging in *in vivo* lung carcinogenesis experiments. In the case of magnetic resonance imaging, it produces high soft-tissue contrast, but takes time to scan the whole animal image. Moreover, a new technology may synergize two imaging methodologies, such as positron emission tomography and CT, for better assessment. This novel approach in the present study may also have an impact on the study of natural lung tumor progression or regression and cancer chemopreventive and therapeutic agents.

Acknowledgments

This work was supported by Grants-in-Aid for Cancer Research, for the Third-Term Comprehensive 10-Year Strategy for Cancer Control from the Ministry of Health, Labour, and Welfare of Japan. Dr Tsukasa Kitahashi and Dr Shuji Yamamoto were the recipients of a Research Resident fellowship from the Foundation for Promotion of Cancer Research during the time of this research.

References

1 Jemal A, Murray T, Ward E *et al*. Cancer statistics 2005. *CA Cancer J Clin* 2005; **55**: 10–30.
2 Mulshine JL. Screening for lung cancer: in pursuit of pre-metastatic disease. *Nat Rev Cancer* 2003; **3**: 65–73.
3 Paulus MJ, Gleason SS, Kennel SJ, Hunsicker PR, Johnson DK. High resolution X-ray computed tomography: an emerging tool for small animal cancer research. *Neoplasia* 2000; **2**: 62–70.
4 Kuhn JL, Goldstein SA, Feldkamp LA, Goulet RW, Jesion G. Evaluation of a microcomputed tomography system to study trabecular bone structure. *J Orthop Res* 1990; **8**: 833–42.
5 De Clerck NM, Meurrens K, Weiler H *et al*. High-resolution X-ray microtomography for the detection of lung tumors in living mice. *Neoplasia* 2004; **6**: 374–9.
6 Cavanaugh D, Johnson E, Price RE, Kurie J, Travis EL, Cody DD. *In vivo* respiratory-gated micro-CT imaging in small-animal oncology models. *Mol Imaging* 2004; **3**: 55–62.
7 Badea C, Hedlund LW, Johnson GA. Micro-CT with respiratory and cardiac gating. *Med Phys* 2004; **31**: 3324–9.
8 Cody DD, Nelson CL, Bradley WM *et al*. Murine lung tumor measurement using respiratory-gated micro-computed tomography. *Invest Radiol* 2005; **40**: 263–9.
9 Li XF, Zanzonico P, Ling CC, O'Donoghue J. Visualization of experimental lung and bone metastases in live nude mice by X-ray micro-computed tomography. *Technol Cancer Res Treat* 2006; **5**: 147–55.
10 Winkelmann CT, Figueroa SD, Rold TL, Volkert WA, Hoffman TJ. Microimaging characterization of a B16-F10 melanoma metastasis mouse model. *Mol Imaging* 2006; **5**: 105–14.
11 Ulrich M. *International Classification of Rodent Tumors: Mouse*. New York: Springer-Verlag, 2001.
12 Nettleship A, Henshaw P, Meyer H. Induction of pulmonary tumors in mice with ethyl carbamate (urethane). *J Natl Cancer Inst* 1943; **4**: 309–19.
13 Lin L, Festing MF, Devereux TR *et al*. Additional evidence that the K-ras protooncogene is a candidate for the major mouse pulmonary adenoma susceptibility (Pas-1) gene. *Exp Lung Res* 1998; **24**: 481–97.